Measurement of the differential thermal expansion and temperature dependence of refractive index in gradient-index glass

Paul O. McLaughlin and Duncan T. Moore

The thermal expansion and temperature dependence of the refractive index in gradient-index glass have been investigated. In an earlier paper [P. O. McLaughlin and D. T. Moore, "Models for the Thermal Expansion Coefficient and Temperature Coefficient of the Refractive Index in Gradient Index Glass," Appl. Opt. 24, this issue (15 Dec. 1985)] these two thermal properties were modeled as functions of the local glass composition within the gradient-index region. In this paper measurements of α_L and dn/dT are described. A modified multiple Fabry-Perot interferometer was designed and built into an environmental temperature chamber to measure these thermal properties in gradient-index glass in the 0–100°C range. The interferometer operated under computer control to measure optically the differential thermal expansion and change in refractive-index profile in several samples of gradient-index glass.

I. Introduction

Thermal expansion and temperature dependence of refractive-index measurements have been performed on a large number of commercial and experimental homogeneous glass types.[1–3] Thermal expansion has been both mechanically[4] and optically[3] measured. Optical interferometry[3] and minimum deviation[5] techniques have been used to measure dn/dT. However, measurements of thermal expansion and dn/dT in gradient-index glass have not been previously reported. The techniques developed for homogeneous glasses which spatially average the information are not applicable to the gradient-index case. For this reason, it was necessary to develop a new instrument which would permit the thermal expansion coefficient and dn/dT to be measured as a function of spatial coordinate. To accomplish this task, a Fabry-Perot interferometric system was designed and built to measure thermal expansion and temperature dependence of refractive index as a function of spatial position within the gradient. The measurements of these thermal properties in the temperature range of 0–100°C were made with the interferometer and gradient-index samples at constant uniform temperature to avoid the effects that thermal gradients would have introduced into the measurement analysis.

Descriptions of the interferometer, the gradient-index samples, and the experiments to determine α_L and dn/dT are presented. Results of the experiments are compared to predictions based on models presented in an earlier paper[6] for α_L and dn/dT in gradient-index glass.

II. Multiple Fabry-Perot Interferometer

A modified multiple plane–parallel plate Fabry-Perot interferometer system was designed and built to measure both thermal expansion and dn/dT as a function of position in a gradient-index glass sample. Samples of gradient-index glass to be measured in the interferometer were fabricated into the geometry illustrated in Fig. 1. The samples had a 1-D index gradient, and the faces of the sample perpendicular to the gradient were polished plane and parallel to each other. Portions of the front and rear faces were coated as shown in Fig. 1. This coating scheme allowed both the thermally induced surface profile changes and the temperature-dependent changes in refractive index to be measured. The gradient-index sample was placed inside a reference plane–parallel Fabry-Perot interferometer (RFP) forming a multiple interferometer as shown in Fig. 2.

In a plane-parallel plate Fabry-Perot interferometer, the optical path between two consecutive interfering beams is

When this work was done both authors were with the University of Rochester, Institute of Optics, Rochester, New York 14627; P. O. McLaughlin is now with Nippon Sheet Glass Company, Central Research Laboratory, Konoike, Itami, Hyogoken 664, Japan.

Received 2 November 1984.
0003-6935/85/244334-08$02.00/0.

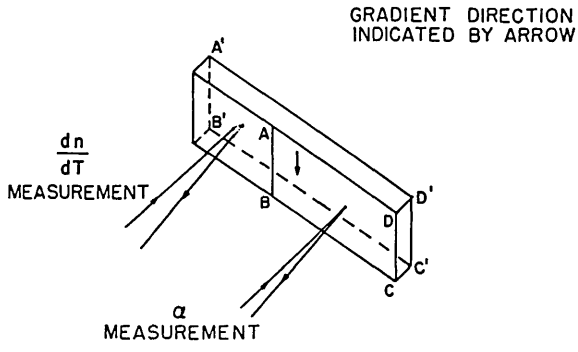

SURFACES POLISHED PLANE PARALLEL, HIGH REFLECTANCE COATINGS ON AREAS ABCD AND A'B'C'D'

Fig. 1. Gradient-index sample preparation.

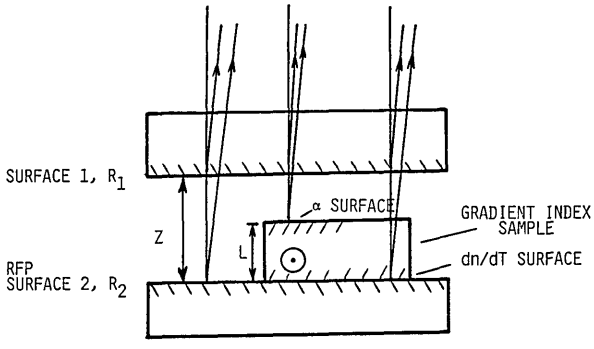

Z = RFP PLATE SEPARATION

L = GRADIENT INDEX SAMPLE THICKNESS

⊙ INDICATES GRADIENT DIRECTION

Fig. 2. Multiple Fabry-Perot interferometer.

$$\mathrm{OPD} = 2nZ, \tag{1}$$

where n is the refractive index of the medium between the plates, and z is the plate separation. In the Fabry-Perot interferometer formed by the upper RFP plate and the upper surface of the gradient-index sample, the optical path was a function of position in the samples that expanded differentially across the gradient region. Similarly, when measuring the gradient refractive-index profile, the index was also a function of position. The optical path difference at a given temperature can be expressed as

$$\mathrm{OPD} = (x,y,T) = 2n_{\mathrm{RFP}}(T)[z(T) - l(x,y,T)] + 2n(x,y,T)l(x,y,T), \tag{2}$$

where n_{RFP} is the refractive index of air, and $n(x,y,T)$ is the refractive index at a point in the gradient-index sample. Equation (2) and subsequent equations for the optical path through the gradient region assume the samples can be treated as simple phase objects in the interferometer. In practice this criterion was met by choosing a low reflectance finesse ($F \sim 4$) for the Fabry-Perot interferometer and by preparing sufficiently thin samples for the index profile measurements. Thicker samples were used to measure the differential thermal expansion.

When the temperature of the multiple interferometer was changed from temperature T_1 to temperature T_2, the change in optical path introduced is given by

$$\begin{aligned}\mathrm{OPD}(x,y,T_1) - \mathrm{OPD}(x,y,T_2) = {} & 2[n_{\mathrm{RFP}}(T_1)z(T_1) - n_{\mathrm{RFP}}(T_2)z(T_2)] \\ & - 2[n_{\mathrm{RFP}}(T_1)l(x,y,T_1) \\ & - n_{\mathrm{RFP}}(T_2)l(x,y,T_2)] \\ & + 2[n(x,y,T_1)l(x,y,T_1) \\ & - n(x,y,T_2)l(x,y,T_2)]\end{aligned} \tag{3}$$

Equation (3) is grouped so that the first term represents the optical path difference that is observed in the reference Fabry-Perot interferometer.

The first two terms in Eq. (3) represent the optical path differences measured between the upper RFP plate and the upper surface of the gradient-index sample. The optical path difference between the upper RFP plate and the second surface of the gradient-index sample is given by all the terms of Eq. (3). The change in refractive-index profile across the gradient region due to the difference in temperature can be determined once the physical thickness of the sample has been determined. As seen in the third term of Eq. (3), it is necessary to determine the sample thickness at each point to separate the optical path difference due solely to the index change with temperature from the total optical path measured. By making these measurements in the multiple Fabry-Perot interferometer, the thermal expansion and temperature-dependent change in refractive index were determined in gradient-index glass.

The multiple Fabry-Perot interferometer system designed and built to make these measurements as a function of spatial coordinate employed a homodyne phase measurement technique that facilitated rapid accurate optical phase data collection by the microcomputer. The computer was not only responsible for the control of the data taking and recording process, but it was also an integral part of the phase detection scheme.

The multiple interferometer utilized a homodyne phase measurement based on the two-detector phase detection technique developed by Moore[7] and Eastman.[8] As a periodic waveform was applied to the piezoelectric transducer (see Fig. 3), the upper Fabry-Perot plate was displaced through a distance greater than half of a wavelength of the laser light source. Since the upper Fabry-Perot plate was common to each interferometer, the optical path difference in all three interferometers changed with time while the relative optical phase at all points in the interferometer was maintained.

The waveform used to drive the piezoceramic transducer (PZT) was generated and stored within the com-

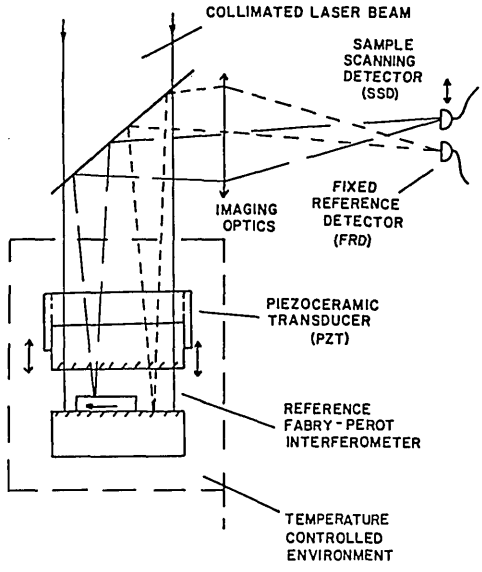

Fig. 3. Multiple Fabry-Perot interferometer system.

puter's memory. The computer was interfaced to the PZT through a digital-to-analog converter and a high voltage operational amplifier. The computer cycled sequentially through the waveform driving the upper Fabry-Perot plate through several 2π optical phase changes. This is illustrated in Fig. 4. The detected intensity signal from each photomultiplier tube (PMT) cycled through more than one complete 2π period in intensity. One detector, the reference detector (FRD), was located at a fixed position in the RFP interference pattern, and a second detector, the scanning sample detector (SSD), was located at a point on the gradient-index glass sample. The relative phase difference between the FRD and SSD detectors was proportional to the optical phase difference between the two points to within an integer number of 2π optical phase differences. Moving the sample detector to a new point on the sample, the detected phase shift relative to the fixed detector mapped the change in either the optical or physical thickness of the sample with position as described by Eq. (2).

The technique for determining the relative phase difference between the temporally varying reference detector signal and sample detector signal, as implemented in the multiple Fabry-Perot interferometer, was highly computer hardware and software oriented. Figure 5 is a block diagram illustrating the hardware interfacing of the computer to the multiple Fabry-Perot interferometer. The computer is interfaced to the PZT through a 10-bit digital-to-analog converter and high voltage operational amplifier to modulate the optical phase in the interferometer. Orthogonal galvanometers under computer control determine the point on the sample to be imaged onto the sample detector. Signals from the two detectors were processed, and digital information sufficient to determine the relative optical phase at the sample detector was sent to the computer. The actual electronic phase detection technique is detailed in Ref. 9. The computer also monitored the temperature at several points around the interferometer.

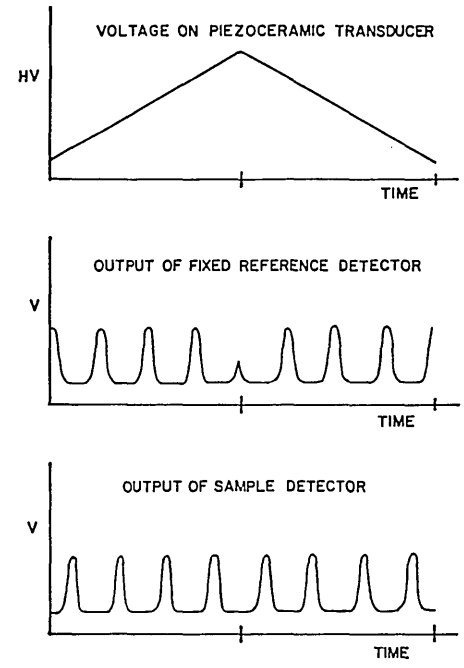

Fig. 4. Phase modulation.

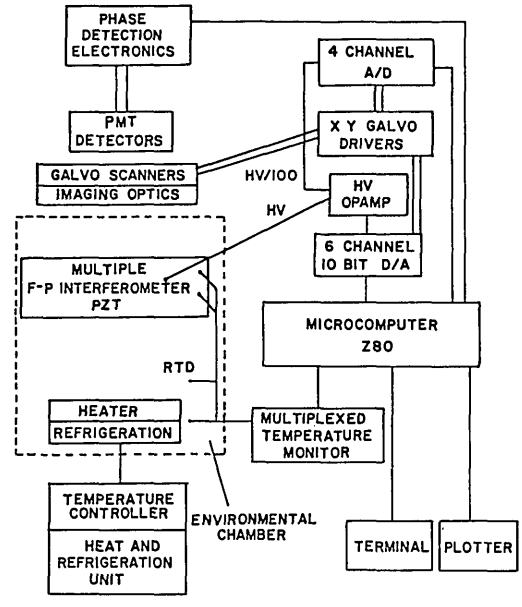

Fig. 5. Computer interfacing.

The optical system is pictured in Fig. 6. A He–Ne laser was used for the light source. The multiple Fabry-Perot interferometer was the only optical component inside the temperature controlled environmental chamber. The imaging optics imaged one point on the gradient-index sample onto the sample detector. To measure the optical phase at a particular point on the sample, the mirrors on the orthogonally mounted galvanometers were rotated under computer control to move the image of that point onto the detector. Imaging a single point onto the detector allowed the optical

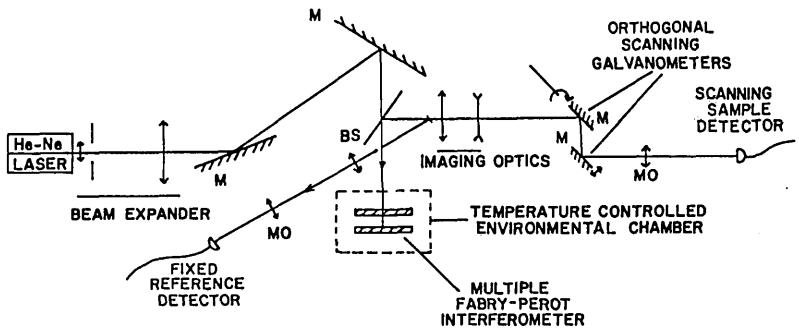

Fig. 6. Optical system.

phase as a function of spatial coordinate to be measured and recorded at each temperature.

III. Gradient-Index Samples

Gradient-index samples for this research were all produced by the ion exchange technique starting with the same type of homogeneous base glass. The base glass was a soda-rich alumina-silicate glass manufactured by Bausch & Lomb Corp.[10] The glass compositon and other physical properties of the glass are given in Table I. A 1-D composition gradient was produced by placing a large diameter disk of the homogeneous base glass into an appropriate molten salt bath.

Table I. Physical Properties Homogeneous Base Glass

Glass composition	Oxide component	Mole %
	SiO_2	69.68
	Al_2O_3	4.53
	Na_2O	25.79
Refractive index	$n = 1.5025 \pm 0.001$ at $\lambda = 0.5893\ \mu m$	
	$n = 1.500 \pm 0.001$ at $\lambda = 0.6328\ \mu m$	
Abbe number	$v = 57.7$	
Absolute dn/dT at $\lambda = 0.6328\ \mu m$ (25–80°C)	$dn/dT = -3.6 \times 10^{-6}$/°C	
Density	$\rho = 2.500$ g/cm	
Thermal expansion coefficient (25–80°C)	$\alpha_L = 11.2 \times 10^{-6}$ mm/mm°C	
Transformation temperature	$T_g = 507$°C	

Diffusion occurred across the glass–salt interface with ions from the glass (exchange ions) diffusing out and ions from the salt (diffusing ions) diffusing into the glass. Samples as illustrated in Fig. 1 were then cut from the disk. The concentration profiles of the exchange ions and the diffusing ions were determined from electron beam microprobe measurements.

Four different gradient-index glasses were investigated. Three glasses were produced at the University of Rochester, and one glass was produced at Bausch & Lomb Corp. as part of joint National Science Foundation research project with the University.[10] Table II is a list of the samples investigated. For each glass type, the exchange ions and diffusing ions are given along with the maximum diffusion depth, maximum exchange parameter, and maximum index change. The exchange parameters, represented by u and v, are defined so that at any point in the glass

$$\left.\begin{aligned} p_{ex}' &= p_{ex}(1-u-v), \\ p_b &= p_{ex}u, \\ p_c &= p_{ex}v, \\ 0 \geq u \geq 1 \quad 0 \geq v \geq 1 \quad 0 \geq u+v \geq 1, \end{aligned}\right\} \tag{4}$$

where p_{ex} and p_{ex}' are mole fractions of the exchange ion component in the glass before and after diffusion, respectively, and p_b and p_c are mole fractions of the diffusing ion components of types b and c in the glass after diffusion.

The exchange parameters were introduced to aid the modeling of α_L and dn/dT in gradient-index glass,[6] The exchange parameters vary as functions of position

Table II. Gradient-Index Glass Samples

Glass designation	Exchange ion	Diffusing ion	Diffusion depth maximum	Exchange parameter maximum	Δn maximum	Sample designation	Sample thickness
BL:Li	Na^+	Li^+	2.6 mm	0.60 ± 0.02	0.0172 ±0.0005	BL:Li1	7.89 mm ±0.015 mm
						BL:Li2	0.51
BL:K	Na^+	K^+	0.6	0.96	0.0011	BL:K1	4.98
						BL:K2	0.62
BL:LiK	Na^+	Li^+	3.0	0.49	0.0109	BL:LiK1	4.94
		K^+	0.5	0.02		BL:LiK2	0.62
BL20	Na^+	Ag^+	6.0	0.08	0.0107	BL20B	2.12
						BL20A	0.62

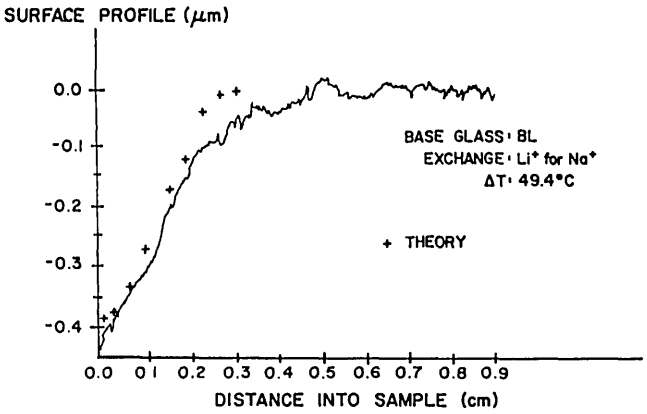

Fig. 7. Change in surface profile for sample BL:Li1.

within the gradient region. These definitions are also consistent with the exchange parameters first introduced by Fantone[11] in his work related to modeling the refractive index in gradient-index glass.

IV. Experimental Measurements and Results

The gradient-index samples were individually tested in the multiple Fabry-Perot interferometer. To avoid effects of thermal gradients influencing the results, measurements across the samples were made only after the sample had reached a constant uniform temperature. Data taken at each temperature were referenced to the edge of the gradient end of the sample. The edge of the sample provided a unique point to which the data could be referenced. Considering that the sample expanded as the temperature was changed, the maximum registration error introduced by referencing data to the edge of the sample was simply the difference in depth to the homogeneous region. Letting z_{max} equal the maximum gradient depth at the initial temperature, the maximum error is $z_{max}\alpha_L\Delta T$. For a 100°C temperature change, this registration error never exceeded 7 μm which was smaller than the spatial resolution of the imaging optics and, therefore, was neglected.

A. Thermal Expansion

The difference in thermal expansion across the gradient-index region of each glass was measured, and the experimental results were compared to the predicted thermal expansion from the model developed for gradient-index glass presented in our earlier paper.[6] The results are presented in two forms. First, the measured change in the surface profile of the sample due to the differential expansion is plotted with a number of corresponding points calculated from the model, and, from the experimental data, a table of thermal expansion coefficients as a function of position within the gradient-index region was generated and compared to the model.

The change in surface profile across the gradient-index region of sample BL:Lil due to a 49.4°C temperature change is presented in Fig. 7. In this sample, lithium ions had partially replaced the sodium ions at one end of the sample. As seen in Fig. 7, the lithium rich end of the sample expanded less than the original base glass. The initial sample temperature was 25.8°C, and the total temperature change was 49.4°C. For this temperature change, the surface change predicted by the model agreed well with the experimental data. The total surface change across the gradient region was 0.42 μm, and the predicted change was 0.38 μm. From Table III, the thermal expansion coefficient is seen to have decreased by 2×10^{-6}/°C across the gradient region. This represents a 19% decrease in the thermal expansion coefficient of the glass.

The differential expansion in gradient-index sample BL:Kl was measured for a 49.6°C temperature change. The initial temperature was 25.8°C. The change in surface profile is plotted in Fig. 8. In this sample, the larger potassium ions introduced for the original sodium ions in the glass resulted in an increase in the thermal expansion across the gradient region. The top trace is plotted on the same scale as the previous sample. The gradient region is rescaled in the bottom plot, and at each point a corresponding value was calculated from the model. In this case, the agreement is excellent. The model's departure from the experimental data was no greater than the noise level in the interferometer. From Table IV, the change in the thermal expansion across the gradient region increased the thermal expansion coefficient of the glass by 15%.

Table III. Differential Thermal Expansion in Sample BL:Li1

Distance into sample (cm)	Exchange parameter u	Differential expansion ($\times 10^{-6}$)		Change in surface profile	
		Predicted	Experiment	Predicted	Experiment
0.0	0.060 ± 0.02	−1.9 ± 0.01/°C	−2.1 ± 0.2/°C	−0.38 ± 0.0 μm	−0.41 ± 0.03 μm
0.02	0.58	−1.9	−2.0	−0.37	−0.38
0.06	0.52	−1.7	−1.7	−0.33	−0.33
0.10	0.41	−1.3	−1.5	−0.26	−0.30
0.14	0.26	−0.8	−1.0	−0.16	−0.19
0.18	0.12	−0.4	−0.7	−0.08	−0.14
0.22	0.04	−0.1	−0.5	−0.03	−0.09
0.26	0.01	−0.0	−0.3	−0.01	−0.07
0.30	0.00	0	−0.2	0.0	−0.04

Initial sample thickness: 0.7890 cm ± 0.0015 cm
Initial temperature: 25.8°C
Temperature change: 49.4°C

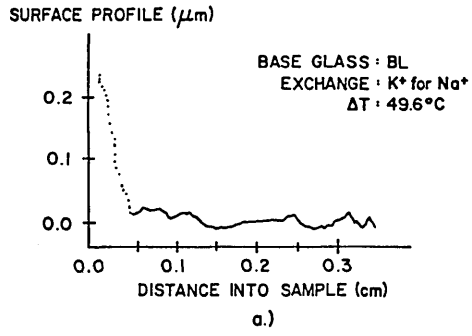

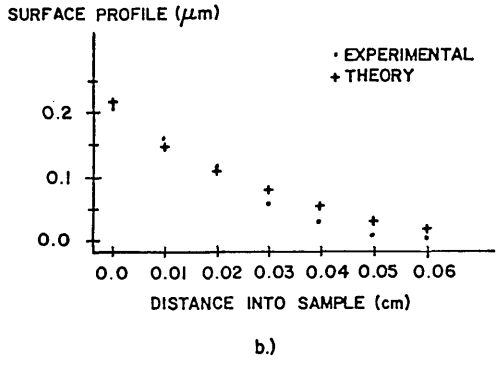

Fig. 8. Change in surface profile for sample BL:K1.

In agreement with the thermal expansion model, these two exchange systems resulted in approximately equal and opposite changes in the thermal expansion coefficients.

Sample BL:LiKl was an attempt to introduce both potassium and lithium ions into sodium aluminosilicate base glass. While the percentage of potassium ions to exchange into the glass was relatively small, the concentration profile of the lithium ions was different from the profile in sample BL:Lil. As seen in Fig. 9 and from Table V, agreement between the model and experimental data is again quite good. The maximum percent change in the thermal expansion coefficient of the glass was −17%.

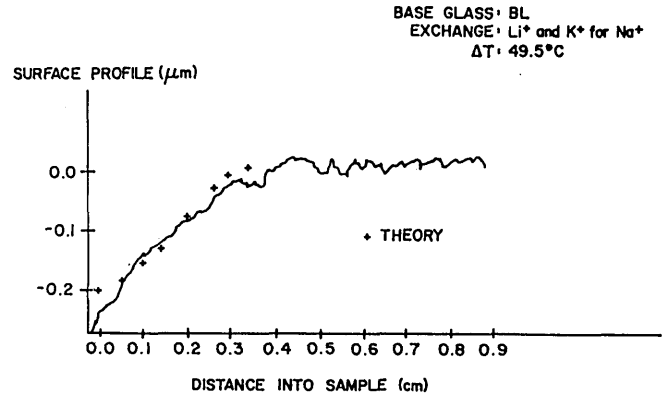

Fig. 9. Change in surface profile for sample BL:LiK1.

Table IV. Differential Thermal Expansion in Sample BL:K1

Distance into sample (cm)	Exchange parameter u	Differential expansion ($\times 10^{-6}$)		Change in surface profile	
		Predicted	Experiment	Predicted	Experiment
0.0	0.96 ± 0.02	1.7 ± 0.1/°C	1.7 ± 0.2/°C	0.22 ± 0.01 μm	0.21 ± 0.03 μm
0.01	0.64	1.2	1.3	0.14	0.16
0.02	0.49	0.9	0.9	0.11	0.11
0.03	0.37	0.7	0.5	0.08	0.06
0.04	0.26	0.5	0.3	0.06	0.03
0.05	0.15	0.3	0.1	0.03	0.01
0.06	0.07	0.1	0.0	0.01	0.0

Initial sample thickness: 0.4980 cm ± 0.0015
Initial temperature: 25.8°C
Temperature change: 49.6°C

Table V. Differential Thermal Expansion in Sample BL:LiK1

Distance into sample (cm)	Exchange parameter		Differential Expansion ($\times 10^{-6}$)		Change in surface profile	
	$u(\pm 0.02)$	$v(\pm 0.02)$	Predicted	Experiment	Predicted	Experiment
0.00	0.49	0.01	−1.6 ± 0.1/°C	−1.9 ± 0.2/°C	−0.19 ± 0.01 μm	−0.23 ± 0.03 μm
0.06	0.45	0	−1.5	−1.5	−0.18	−0.18
0.10	0.40	0	−1.3	−1.2	−0.16	−0.14
0.14	0.33	0	−1.1	−1.0	−0.13	−0.12
0.18	0.24	0	−0.8	−0.7	−0.10	−0.08
0.22	0.16	0	−0.5	−0.6	−0.06	−0.07
0.26	0.08	0	−0.3	−0.3	−0.03	−0.04
0.30	0.02	0	−0.1	−0.2	−0.01	−0.02

Initial sample thickness: 0.4940 cm ± 0.0015 cm
Initial temperature: 25.8°C
Temperature change: 49.5°C

In the fourth sample, BL20B, silver ions were diffused into the base glass replacing sodium ions. The refractive-index gradient was obtained by replacing a maximum of 7% of the sodium ions from the base glass. For a 50°C temperature change and measuring to the nearest $\lambda/20$ (0.03 μm), no change in the surface profile could be detected. For this sample, the maximum change in thermal expansion coefficient across the gradient region was less than

$$|\delta\alpha_L| < 0.6 \times 10^{-6}/°C. \quad (5)$$

To compare this change in thermal expansion to the model, the predicted change is given by

$$\delta\alpha_L = (\alpha_{Ag} - \alpha_{Na})P_{Na}u, \quad (6)$$

where α_{Ag} and α_{Na} are the partial linear expansion factors for silver oxide and sodium oxide in the glass, respectively, P_{Na} is the original mole fraction of Na_2O in the glass, and u is the exchange parameter. The value of the partial linear expansion factor for sodium oxide is $39.5 \times 10^{-6}/°C$. Silver oxide, Ag_2O, is not a common glass component so its additive factor had to be approximated using the relationship between the partial factors and the reciprocal of the ionic field strength of the oxide as described in Ref. 6. Using this relationship, the partial linear expansion factor for silver oxide is $\sim 45 \times 10^{-6}/°C$. Substituting these values into Eq. (6), the predicted change in α_L for sample BL20B is $0.1 \times 10^{-6}/°C$. Comparing the experimental and predicted change, it is clear that to confirm the contribution of silver oxide to the thermal expansion in gradient glass it is necessary to increase the accuracy of the measurement by an order of magnitude. However, the experiment has pointed out that if the desired change in refractive index is obtained by replacing only a small percentage of the original ions in the glass, it is less critical that the partial linear expansion factors of the two oxides be the same.

B. Temperature Dependence of Refractive Index

To determine the change in the temperature coefficient of refractive index across the gradient-index region, the total optical path through the gradient-index glass as a function of spatial coordinate was measured at two different temperatures for each thin sample. The expression for the change in optical path as a function of position for two different temperatures, given in Eq. (3), can be rewritten in terms of the parameter values at temperature T_1 and the spatially dependent thermal coefficients, $\alpha_L(x,y)$ and $dn(x,y,)/dT$, of the gradient-index sample:

$$\begin{aligned}\mathrm{OPD}(x,y,T_1) - \mathrm{OPD}(x,y,T_2) &= 2[n_{RFP}(T_1)z(T_1) - n_{RFP}(T_2)z(T_2)] \\ &- 2\left\{n_{RFP}(T_1)l(x,y,T_1) - \left[n_{RFP}(T_1) + \frac{dn_{RFP}}{dT}\Delta T\right] l(x,y,T_1)(1 + \alpha_L(x,y)\Delta T)\right\} \\ &+ 2\left\{n(x,y,T_1)l(x,y,T_1) - \left[n(x,y,T_1) + \frac{dn}{dT}(x,y)\Delta T\right] l(x,y,T_1)(1 + \alpha_L(x,y)\Delta T)\right\}. \quad (7)\end{aligned}$$

Measurements were made on the samples at a constant uniform temperature, and only the spatially dependent terms of Eq. (7) contributed to the change in dn/dT across the gradient. For the plane-parallel samples, $l(x,y,T_1)$ can be set to l_1. Retaining only the first-order spatially dependent terms and solving for the temperature coefficient of refractive index at a point in the gradient,

$$\frac{dn(x,y)}{dT} = -\frac{1}{2l_1\Delta T}[\mathrm{OPD}(x,y,T_1) - \mathrm{OPD}(x,y,T_2)] - [n(x,y) - n_{RFP}]\alpha_L(x,y). \quad (8)$$

The refractive-index profile, $n(x,y)$, in this case was a 1-D gradient and was obtained by adding the base glass index to the temperature T_1 gradient-index profile. The index profile for sample BL:LiK2 is shown in Fig. 10. Similarly, $\alpha_L(x,y)$ is the sum of the base glass expansion coefficient, and the change in that coefficient as measured and recorded in Tables III–V.

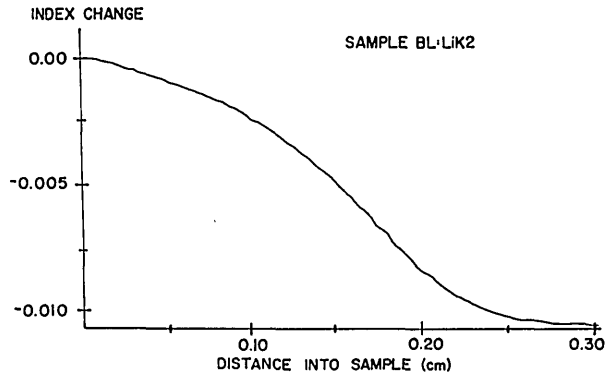

Fig. 10. Gradient-index profile for sample BL:LiK2.

Each of the four thin gradient-index samples was measured at room temperature and at ~50°C above room temperature. Sample BL20A was also measured at −1°C. Table VI lists the experiments performed and summarizes the results of the optical path difference measurements at each temperature. The maximum change in optical path for each sample did not vary by more than 0.1 wavelengths for the given temperature change. However, the uncertainty in relating the data between the two temperatures is $\sim 0.2\lambda$. The additional uncertainty arises from subtracting the different background tilts from the two data sets and the uncertainty in registering the data to the exact edge of the sample twice. To the accuracy of the experiment Eq. (8) can be written as

$$\frac{dn(x,y)}{dT} = [n_{RFP} - n(x,y)]\alpha_L(x,y) \pm \frac{1}{2l_1\Delta T}(\lambda/5), \quad (9)$$

where λ is 0.6328 μm and $n_{RFP} = n_{air} = 1$. The change in dn/dT from the homogeneous region of the glass to the edge of the gradient was calculated from Eq. (9)

Table VI. Gradient-Index Measurement

Sample	Temperature (°C)	ΔT (°C)	Maximum OPD $\lambda = 0.6328\ \mu m$
BL:Li2	25.6		$27.8 \pm 0.1\lambda$
		53.3	
	78.9		27.8
	25.9		27.8
		53.4	
	79.3		27.6
BL:K2	25.6		2.2
		53.5	
	78.9		2.0
BL:LiK2	25.3		21.4
		53.9	
	79.2		21.4
BL20A	−1.0		21.0
		28.0	
	27.0		21.0
		52.1	
	79.1		21.0

Table VII. Temperature Dependence of Refractive Index in Gradient-Index Glass

BL base glass dn/dT (25–80°C) -3.6×10^{-6}/°C
Calculated dn/dT (25–40°C) -2.5×10^{-6}/°C

	Change in dn/dT across the gradient-index region	
Sample	Predicted (20–40°C)	Experimental (25–80°C)
BL:Li2	$+1.6 \times 10^{-6}$/°C	$+0.90 \pm 2.4 \times 10^{-6}$/°C
BL:K2	−4.8	-0.86 ± 1.9
BL:LiK2	+1.3	$+0.85 \pm 1.9$
BL20A	−0.3	$<-0.18 \pm 2.0$

using the experimental values of the gradient-index profile at temperature T_1 and the change in α_L across the gradient from the differential expansion measurements.

The results are presented in Table VII and compared to the model for dn/dT in gradient-index glass.[1,9] Three of the four predicted values for the change in dn/dT are within reasonable agreement with the experimental results. The model and experiment are not in agreement for the potassium for sodium exchange in sample BL:K2. This sample should be remeasured to either confirm or reject this set of experimental data. Preferably, another sample should also be fabricated and tested.

V. Conclusions

The measurements of the differential expansion and the change in dn/dT in the gradient-index glass samples have shown the need to consider the thermal properties of gradient-index glass. The experiments have also shown that the models presented in our earlier paper[6] can be used with a reasonable degree of accuracy to predict the thermal properties as a function of position in gradient-index glass. Nevertheless, the samples measured in these experiments do not represent even a small fraction of the number of possible gradient-index glass combinations. It is important that additional measurements be made on other glasses containing other oxides such as the oxides of cesium, rubidium, and thallium.

Finally, the thermal properties of gradient-index materials other than glass should be investigated. Examples of other gradient-index materials currently include gradient-index IR transmitting materials[12] and plastics.[13]

References

1. R. M. Waxler, G. W. Cleek, I. H. Malitson, M. J. Dodge, and T. A. Hahn, "Optical and Mechanical Properties of Some Neodymium-Doped Laser Glasses," J. Res., Res. Nat. Bur. Stand. Sect. A **75,** 163 (1971).
2. J. H. Wray and J. T. Neu, "Refractive Index as Function of Wavelength," J. Opt. Soc. Am. **59,** 774 (1969).
3. Fred A. Molby, "Index of Refraction and Coefficients of Expansion of Optical Glasses at Low Temperatures," J. Opt. Soc. Am. **39,** 600 (1949).
4. Perkin-Elmer Thermo-Mechanical Analyzer model TMS-1.
5. L. W. Tilton, "Standard Conditions for Precise Prism Refractometry," J. Res. Nat. Bur. Stand. **14,** 393 (1935).
6. P. O. McLaughlin and D. T. Moore, "Models for the Thermal Expansion Coefficient and Temperature Coefficient of the Refractive Index in Gradient Index Glass," Appl. Opt. **24,** this issue (15 Dec. 1985).
7. D. T. Moore, "Gradient Index Optics: Aspects of Design, Testing, Tolerancing, and Fabrication," Ph.D. Thesis, U. Rochester, New York (1974).
8. J. M. Eastman, "Surface Scattering in Optical Interference Coatings," Ph.D. Thesis, U. Rochester, New York (1974).
9. P. O. McLaughlin, "Thermal Expansion and Temperature Dependence of the Refractive Index in Gradient Refractive Index Glass," Ph.D. Thesis, U. Rochester, New York (1982).
10. D. T. Moore, "Gradient-Index Optical Glass Lenses," National Science Foundation Research Contract ENG. 74-11993-AO1, Annual Report (1976).
11. S. D. Fantone, "Design, Engineering, and Manufacturing Aspects of Gradient Index Optical Components," Ph.D. Thesis, U. Rochester, New York (1979).
12. J. J. Miceli, "Infrared Gradient Index Optics: Materials, Fabrication, and Testing," Ph.D. Thesis, U. Rochester, New York (1982).
13. Y. Koike and Y. Ohtsuka, "Studies on the Light-Focusing Plastic Rod. 15: GRIN Rod Prepared by Photocopolymerization of a Ternary Monomer System." Appl. Opt. **22,** 418 (1983).

The authors want to acknowledge Burleigh Instruments, Inc., for donating the Fabry-Perot that was modified for these experiments and the National Science Foundation for their financial support of this research (ECS-8106941).

This paper is based on one presented at the Fourth Topical Meeting on Gradient-Index Optical Imaging Systems, held in Kobe, Japan, 4–5 July 1983.